

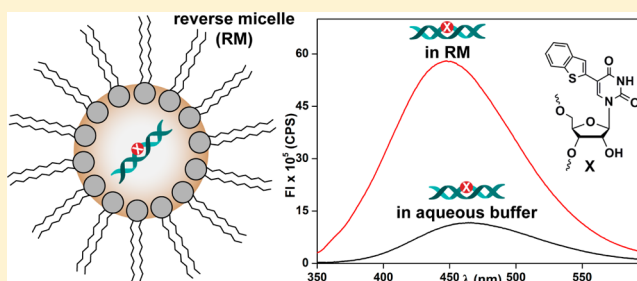
Environment-Responsive Fluorescent Nucleoside Analogue Probe for Studying Oligonucleotide Dynamics in a Model Cell-like Compartment

Maroti G. Pawar and Seergazhi G. Srivatsan*

Department of Chemistry, Indian Institute of Science Education and Research, Pune, Dr. Homi Bhabha Road, Pashan, Pune 411008, India

S Supporting Information

ABSTRACT: The majority of fluorescent nucleoside analogue probes that have been used in the *in vitro* study of nucleic acids are not suitable for cell-based biophysical assays because they exhibit excitation maxima in the UV region and low quantum yields within oligonucleotides. Therefore, we propose that the photophysical characterization of oligonucleotides labeled with a fluorescent nucleoside analogue in reverse micelles (RM), which are good biological membrane models and UV-transparent, could provide an alternative approach to studying the properties of nucleic acids in a cell-like confined environment. In this context, we describe the photophysical properties of an environment-sensitive fluorescent uridine analogue (**1**), based on the 5-(benzo[*b*]thiophen-2-yl)pyrimidine core, in micelles and RM. The emissive nucleoside, which is polarity- and viscosity-sensitive, reports the environment of the surfactant assemblies via changes in its fluorescence properties. The nucleoside analogue, incorporated into an RNA oligonucleotide and hybridized to its complementary DNA and RNA oligonucleotides, exhibits a significantly higher fluorescence intensity, lifetime, and anisotropy in RM than in aqueous buffer, which is consistent with the environment of RM. Collectively, our results demonstrate that nucleoside **1** could be utilized as a fluorescent label to study the function of nucleic acids in a model cellular milieu.



INTRODUCTION

Nucleic acids carry out their functions by interacting with nucleic acids, proteins, and small-molecule metabolites, and during such processes, they often undergo significant conformational changes. Numerous biophysical tools have been developed to investigate these conformational changes and hence the dynamics and binding properties of nucleic acids *in vitro*.^{1–10} Biophysical probes, in particular, fluorescent nucleoside analogues that closely resemble natural nucleosides and photophysically report conformational changes, have been instrumental in studying the dynamics and function of various nucleic acid motifs.^{11–17} Some examples include (a) the detection of single nucleotide polymorphism (SNP)^{18–23} and DNA and RNA lesions,^{24–27} (b) monitoring of nucleic acid structural dynamics,^{28–30} (c) the determination of binding affinities of therapeutically relevant nucleic acid–protein and nucleic acid–small molecule complexes,^{31–35} and (d) the analysis of the electron-transfer process in nucleic acids.^{36,37} However, the excitation maximum in the UV region and low quantum yields when incorporated into oligonucleotides have substantially limited the applications of the majority of fluorescent nucleoside analogues to *in vitro* systems only.¹⁴ Interestingly, comparative studies in aqueous buffers and in membrane models, mimicking the physical properties and crowding that exist in a cellular environment, indicate that the

structure, dynamics, activity, and recognition properties of biological macromolecules depend on the environment in which they are present.^{38–42} Therefore, a fundamental understanding of the behavior of oligonucleotides in a model cellular milieu could provide new insights into nucleic acid folding and recognition properties, which may have implications for the discovery of drugs and diagnostic tools.

In general, water encapsulated in RM of amphiphilic surfactants, which resembles confined water in biological systems, has been used as a very good experimental model for studying the structure, dynamics, and function of biopolymers in a cell-like compartment.^{43–52} One of the well-characterized RM-forming surfactants, AOT (aerosol OT, dioctyl sodium sulfosuccinate), has the ability to solubilize substantial amounts of water in various nonpolar solvents.^{53,54} RM formed by a ternary mixture of water/AOT/apolar solvent consists of nanometer-sized water droplets or water pools surrounded by surfactant molecules in such a way that the polar head groups are oriented toward the surface of the water pool and nonpolar tails are projected out toward the organic bulk phase (Figure 1). It has been well documented that the size of

Received: July 18, 2013

Revised: September 23, 2013

Published: October 25, 2013

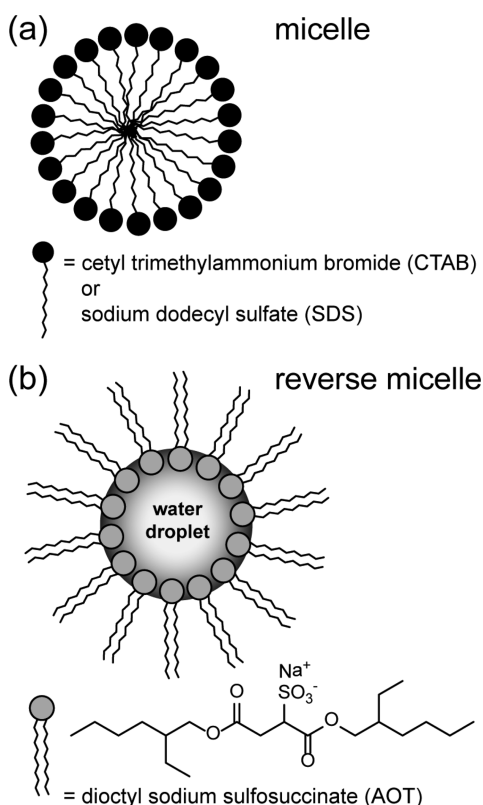


Figure 1. Schematic representations of (a) a micelle and (b) a reverse micelle.

the aqueous micellar core increases linearly with w_0 ($w_0 = [\text{water}]/[\text{AOT}]$),⁵⁵ resulting in variations in the physical properties of the entrapped water such as dynamics,^{56,57} polarity,^{58,59} viscosity,⁶⁰ and proton-transfer efficiency.^{61,62} Attempts have been made to investigate the folding process of nucleic acids of varying masses (30–2700 kDa) in RM.^{63–69} UV absorption, fluorescence, and circular dichroism (CD) measurements revealed that nucleic acids in RM are condensed. Goto and co-workers utilized the slower hybridization rates of DNA in RM to detect the presence of mismatched base pairs in DNA duplexes.⁷⁰ More recently, Flynn and Workman compared the conformational flexibility of two functionally important hairpin RNA motifs, HIV TAR and U4 snRNA, by NMR in RM and aqueous buffer.⁷¹ Their results indicated that confinement restricted the conformational flexibility of both RNA motifs. On the basis of these reports, we envisioned that the photophysical characterization of oligonucleotides labeled with an environment-sensitive fluorescent nucleoside analogue probe in AOT RM would provide an alternative approach to studying the structural dynamics and functions of oligonucleotides in a model cell-like confined environment. Such an endeavor would expand the scope of applications of fluorescent nucleoside analogue probes in general.

We have recently reported the synthesis and photophysical properties of environment-sensitive fluorescent ribonucleoside analogue **1** derived by attaching the benzothiophene moiety at the 5 position of uridine (Figure 2).⁷² This analogue shows emission in the visible region with a reasonable quantum yield and also photophysically responds to solvent polarity changes. Furthermore, the ribonucleoside analogue, when incorporated into oligoribonucleotides, minimally perturbs the structure and photophysically responds to changes in its neighboring base

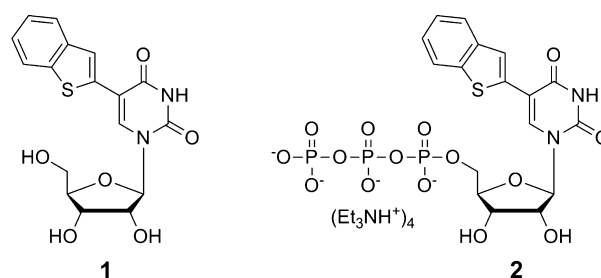


Figure 2. Structure of 5-benzothiophene-conjugated uridine **1** and corresponding triphosphate **2**.⁷²

environment. Hence, we envisaged that the responsiveness of benzothiophene-modified ribonucleoside **1** to changes in its environment could be aptly utilized in studying the properties of oligonucleotides in RM. Here, we describe the photophysical properties of emissive ribonucleoside **1** in micelles and AOT RM as a function of surfactant concentration and water loading, respectively. Rewardingly, the ribonucleoside analogue reports the environment of these surfactant assemblies via changes in its fluorescence properties such as emission maximum, quantum yield, lifetime, and anisotropy. Furthermore, the photophysical characterization of the nucleoside analogue incorporated into oligonucleotides illustrates the potential of the emissive nucleoside as an efficient probe for studying the structural dynamics and function of nucleic acids in RM.

EXPERIMENTAL SECTION

Materials. Cetyltrimethylammonium bromide (CTAB) and diethyl sodium sulfosuccinate (AOT) were obtained from Sigma-Aldrich. AOT was dried under vacuum for 48 h before use. Sodium dodecyl sulfate (SDS) and *n*-heptane (HPLC grade) were obtained from SRL India Limited and RANKEM India, respectively. Benzothiophene-modified RNA oligonucleotide **3** was prepared by in vitro transcription reactions according to our earlier report.⁷² Synthetic oligonucleotides **4** and **5** purchased from Integrated DNA Technologies, Inc. and Dharmacon RNAi Technologies were purified by polyacrylamide gel electrophoresis (PAGE) under denaturing conditions. Millipore water or autoclaved water was used in all spectroscopic measurements.

Instruments. Absorption spectra were recorded on PerkinElmer, Lambda 45, and Shimadzu UV-2600 UV–vis spectrophotometers. Steady-state fluorescence experiments were carried out in a microfluorescence cuvette (Hellma, path length 1.0 cm) on either a Fluorolog-3 (Horiba Jobin Yvon) or Fluoromax-4 spectrophotometer (Horiba Jobin Yvon). Time-resolved fluorescence experiments were performed on a TCSPC instrument (Horiba Jobin Yvon, Fluorolog-3).

Fluorescence Properties of Ribonucleoside **1 in Anionic and Cationic Micelles. Steady-State Fluorescence Measurements.** Aqueous solutions of various concentrations of surfactants (SDS and CTAB) containing ribonucleoside **1** (5 μM) and DMSO (0.5%) were excited at 318 nm. The excitation and emission slit widths were maintained at 2 and 6 nm, respectively. A spectral blank in the absence of emissive ribonucleoside at a respective surfactant concentration was subtracted from each sample spectrum. Fluorescence experiments were performed in triplicate in a microfluorescence cell at 24 °C. Plots of fluorescent intensity at 465 nm versus surfactant concentration were fitted using a sigmoid function of the Boltzmann type (OriginPro 8.5.1, eq 1) to determine the

Table 1. Photophysical Properties of Ribonucleoside 1 in Different Solvents^{72,75,76}

solvent	$E_T(30)^{77}$ (kcal mol ⁻¹)	$\lambda_{\max 1}$ (nm)	$\lambda_{\max 2}$ (nm)	λ_{em} (nm)	ϕ^a	τ_{av} (ns) ^a	$r^{a,b}$
water	63.1	274	318	462	0.035	1.07	0.037
methanol	55.4	274	321	446	0.047	0.60	
dioxane	36.0	275	322	435	0.060	0.45	
ethylene glycol	53.8	275	322	450	0.103	1.68	0.167
glycerol	57.0	275	322	454	0.139	2.02	0.308

^aStandard deviations for quantum yield (Φ), average lifetime (τ_{av}), and anisotropy (r) are ≤ 0.003 , 0.02 ns, and 0.005, respectively. ^b r values reported here are blank uncorrected.

cmc values of SDS and CTAB.^{73,74} For all plots, the χ^2 (goodness of fit) values were very close to unity.

$$y = \frac{A_1 - A_2}{1 + \exp\left(\frac{x - x_0}{\Delta x}\right)} + A_2 \quad (1)$$

where y is the fluorescence intensity at 465 nm, x is the surfactant concentration, x_0 is the center of the sigmoid (cmc), Δx is the slope factor, A_1 is the upper limit of fluorescence intensity, and A_2 is the fluorescence intensity in the absence of surfactant.

Steady-State Fluorescence Anisotropy Measurements. Steady-state fluorescence anisotropy measurements in various solvents were performed on a Fluoromax-4 spectrophotometer (Horiba Jobin Yvon) at 24 °C. Samples (5 μM) were excited at 318 nm, and the emission intensity was collected at the respective emission maximum. The anisotropy value (r) was determined by analyzing the data using software provided with the instrument. Anisotropy measurements were performed in triplicate, and each value reported in this study is an average of 10 successive measurements for each sample.

Time-Resolved Fluorescence Measurements. Excited-state decay kinetics analysis of aqueous solutions of ribonucleoside 1 (5 μM) at varying surfactant concentrations was performed on the TCSPC instrument. The samples were excited using a 339 nm diode laser source (IBH, UK, NanoLED-339L) with a band pass of 10 nm, and the fluorescence signal at the respective emission maximum was collected. Lifetime measurements were performed in triplicate, and decay profiles were analyzed using IBH DAS6 analysis software. The χ^2 (goodness of fit) values were found to be very close to unity for all decay profiles.

Fluorescence Properties of Ribonucleoside 1 in AOT RM. AOT RM in *n*-heptane with increasing w_0 values were prepared by adding appropriate volumes of the nucleoside stock solutions in water such that the concentrations of nucleoside 1 and AOT were maintained at 5 μM and 200 mM, respectively. The samples were prepared in glass vials, sonicated for ~ 20 s, and then equilibrated for 30 min before fluorescence measurements were carried out.

Steady-State Fluorescence Measurements. Samples were excited at 322 nm with an excitation slit width of 3 nm and an emission slit width of 5 nm. A spectral blank at respective w_0 value in the absence of ribonucleoside was subtracted from each sample spectrum. Fluorescence experiments were performed in triplicate in a microfluorescence cell at 24 °C.

Time-Resolved Fluorescence Measurements. Excited-state decay kinetics analysis of ribonucleoside 1 (5 μM) in AOT RM as a function of w_0 was performed by exciting the samples using 339 nm diode laser source (IBH, UK, NanoLED-339L) with a band pass of 6 nm. The fluorescence signal at the emission maximum was collected. Lifetime measurements were performed in triplicate, and decay profiles were analyzed

using IBH DAS6 analysis software. Fluorescence intensity decay profiles at different w_0 values were found to be triexponential with χ^2 (goodness of fit) values very close to unity.

Fluorescence Properties of Oligoribonucleotide 3 and Duplexes Made of 3 in AOT RM. Stock solutions of 3 and duplexes 3-4 and 3-5 (28 μM) were prepared by annealing a 1:1 mixture of the respective oligonucleotides in 20 mM cacodylate buffer (pH 7.6, 50 mM NaCl, 0.5 mM EDTA) at 90 °C for 3 min and cooling the samples slowly to room temperature. The samples were stored at ~ 4 °C overnight before use. An appropriate volume of the oligonucleotide stock was added to the AOT RM in heptane such that the w_0 value and concentration of the oligonucleotide and AOT were maintained at 20, 2 μM and 200 mM, respectively. The samples were sonicated for nearly 5 s and then equilibrated for 30 min. Steady-state fluorescence measurements were performed in duplicate (24 °C) by exciting the samples at 322 nm with excitation and emission slit widths of 3 and 8 nm, respectively. A spectral blank of AOT RM at $w_0 = 20$ in the absence of oligonucleotides was subtracted from each sample spectrum. Time-resolved fluorescence measurements were performed by exciting the samples using 320 nm diode laser source (IBH, UK, NanoLED-320L) with a band pass of 2 nm, and the fluorescence signal was collected at the respective emission maximum. The decay profiles were analyzed using IBH DAS6 analysis software. The χ^2 (goodness of fit) values were found to be very close to unity for all decay profiles. The fluorescence properties of 3 and duplexes 3-4 and 3-5 (2 μM) were also evaluated in aqueous buffer (20 mM cacodylate, pH 7.6, 50 mM NaCl, 0.5 mM EDTA) under similar conditions by following the above procedure.

RESULTS AND DISCUSSION

Photophysical Properties of Ribonucleoside 1 in Solvents of Different Polarity and Viscosity. Preliminary photophysical characterizations in solvents of different polarity and viscosity indicated that nucleoside analogue 1 could be utilized in studying the polarity and viscosity changes that occur in micellar systems.^{72,75} The ribonucleoside analogue showed two distinct absorption maxima (274 and 318 nm), which were marginally affected by changes in solvent polarity (Table 1). However, the fluorescence properties of nucleoside 1 were found to be affected significantly by solvent polarity changes. Although a solution of nucleoside in water, when excited at its lowest-energy maximum, displayed emission in the visible region ($\lambda_{\text{em}} = 462$ nm) with a quantum yield of 3.5% and a lifetime of 1.07 ns, a solution of nucleoside in dioxane displayed a blue-shifted emission ($\lambda_{\text{em}} = 435$ nm) with an enhanced quantum yield of 6.0% and a shorter lifetime of 0.45 ns.⁷² A solution of nucleoside 1 in ethylene glycol ($\eta_{25^\circ\text{C}} = 16.1$ cP) showed a blue-shifted emission maximum corresponding to a

nearly 3-fold enhancement in fluorescent intensity as compared to that in water ($\eta_{25^\circ\text{C}} = 0.9$ cP, Figure 3, Table 1). When

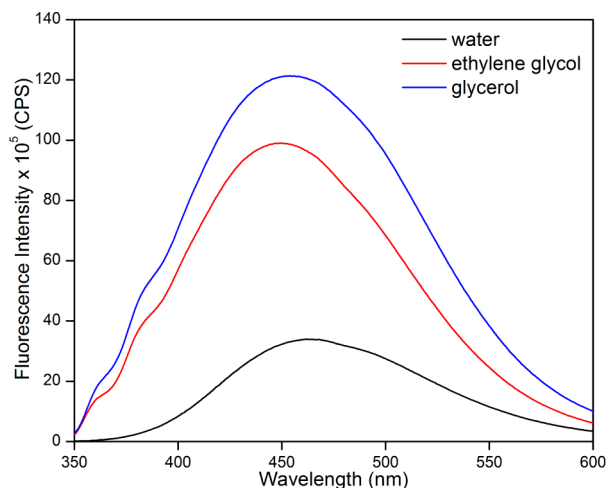


Figure 3. Emission spectra of ribonucleoside **1** ($5\ \mu\text{M}$) in solvents of different viscosity. The ribonucleoside was excited at 318 nm (water) and 322 nm (ethylene glycol and glycerol). Excitation and emission slit widths were 4 and 6 nm, respectively.

measured in a more viscous solvent, glycerol ($\eta_{25^\circ\text{C}} = 934$ cP), a further enhancement in fluorescence intensity was observed with no apparent change in the emission maximum because the polarities of ethylene glycol and glycerol are similar. Furthermore, as the solvent viscosity was increased, the nucleoside exhibited a longer lifetime and greater anisotropy as a result of the rigidification of the chromophore in a viscous solvent compared to the same parameters in a less-viscous solvent (Table 1, Figure S1).

The solvent dipolar relaxation process can affect the emission maximum of a polar fluorophore upon excitation at the red edge of the absorption band.^{78,79} The dipolar relaxation process can be studied by performing a red-edge excitation shift (REES) experiment in which the fluorophore excited at the red edge of the absorption band results in the shift of the emission maximum to longer wavelengths. Typically, the REES effect is observed when a fluorophore is in a motionally restricted environment (e.g., viscous solvents, micelles, liposomes, and

proteins) in which the rate of solvent relaxation is comparable to the lifetime of the fluorophore.^{78–83} Hence, REES can be used as a marker for probing the dynamics of a solvent and the environment of a fluorophore. To study the dependence of the emission maximum on the excitation wavelength, we examined the emission profile of ribonucleoside **1** in glycerol. Upon increasing the excitation wavelength from 310 nm to the red edge of the absorption spectrum (380 nm), we observed a discernible red shift (10 nm) in the emission maximum, which resembles the solvent-relaxed emission profile in water (Figure S2). This result indicates that ribonucleoside **1**, which exhibits a solvent dipolar relaxation process, can be potentially used as a probe to study the dynamics and polarity of its immediate environment in a motionally restricted medium.

Fluorescence Properties of Ribonucleoside **1 in Anionic and Cationic Micelles.** Surfactants such as SDS and CTAB in aqueous solutions form micellar aggregates above a certain concentration called the critical micelle concentration (cmc, Figure 1). The physical properties (e.g., polarity and viscosity) of surfactant solutions above and below the cmc are significantly different, and hence fluorescent probes that interact with specific domains of micelles have been utilized in understanding the morphology and aggregation mechanism and determining the physical properties of micelles.^{84–88} Pyrene and its derivatives, prodan and coumarin dyes, are some of the commonly used probes in the determination of the cmc of surfactant solutions.^{84–88} Consequently, these studies prompted us to evaluate the usefulness of benzothiothiophene-conjugated uridine **1** in monitoring the aggregation process of the surfactant solutions. The emission spectrum of **1** has been recorded in aqueous solutions of anionic (SDS) and cationic (CTAB) surfactants. The nucleoside in an aqueous solution containing SDS at a concentration well below its cmc shows an emission band similar to that in water (Figure 4a). As the concentration of SDS is increased, there is a significant increase in fluorescence intensity, which saturates at high concentrations of the surfactant. A similar trend is also observed when the fluorescence of nucleoside **1** is measured in aqueous solutions containing increasing concentration of CTAB (Figure 5a). A plot of intensity at $\lambda_{\text{em}} = 465$ nm as a function of surfactant concentration gave a typical sigmoidal profile for both surfactants (Figures 4b and 5b). The cmc of SDS (9.3 ± 0.2 mM) and CTAB (0.96 ± 0.01 mM) determined from these

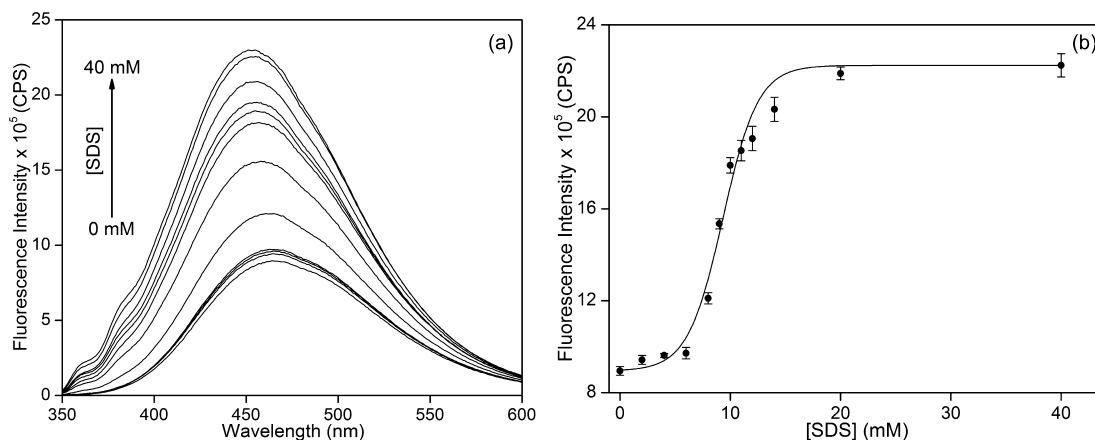


Figure 4. (a) Emission spectra of aqueous solutions of ribonucleoside **1** ($5\ \mu\text{M}$) containing increasing concentrations of SDS. Samples were excited at 318 nm, and excitation and emission slit widths were 2 and 6 nm, respectively. (b) Plot of fluorescence intensity of **1** at 465 nm as a function of SDS concentration.⁷⁵

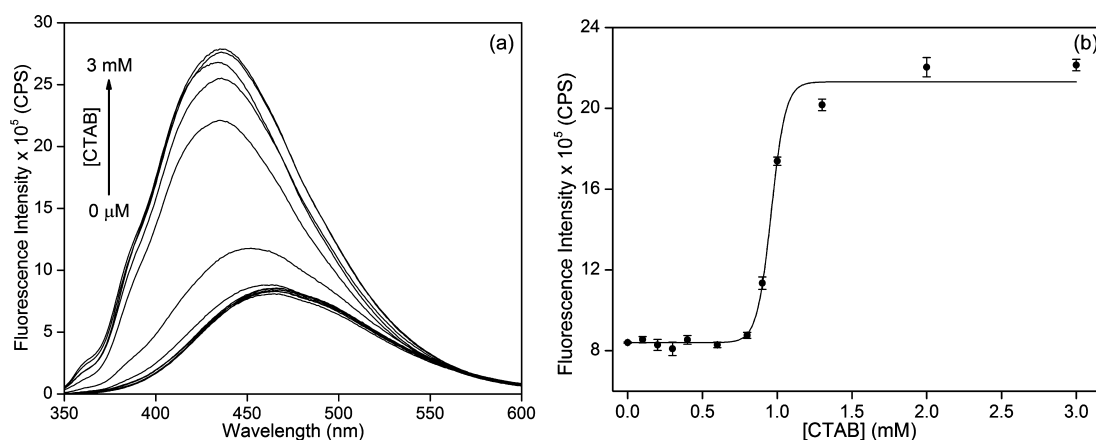


Figure 5. (a) Emission spectra of aqueous solutions of ribonucleoside **1** ($5 \mu\text{M}$) containing increasing concentrations of CTAB. Samples were excited at 318 nm, and excitation and emission slit widths were 2 and 6 nm, respectively. (b) Plot of fluorescence intensity of **1** at 465 nm as a function of CTAB concentration.⁷⁵

plots have been found to be in reasonable agreement with the literature reports (8.0–8.5 and 0.92–1.1 mM, respectively).^{73,89}

A significant increase in fluorescence intensity accompanied by a small spectral shift toward the blue region upon increasing the concentration of the surfactant above the cmc can be explained as follows. At low surfactant concentrations, the emissive nucleoside is solubilized in a more-polar, less-viscous aqueous medium and hence shows quenched emission. This observation is in agreement with the behavior of the nucleoside in solvents of different polarity and viscosity (Table 1). Upon increasing the concentration of the surfactants to above the respective cmc values, the nucleoside gets solubilized in less-polar, more-rigid micellar aggregates, resulting in an enhancement of the fluorescence intensity. Excited-state decay kinetics analysis indicates that the environment around the fluorophore is distinctly different at surfactants concentration below and above respective cmc values (Table 2 and Figure S3).

Table 2. Excited-State Lifetime and Fluorescence Anisotropy of Ribonucleoside **1 ($5 \mu\text{M}$) in SDS and CTAB.⁷⁵**

surfactant	[surfactant] (mM)	τ_{av} (ns) ^a	$r^{a,b}$
SDS	4.0	1.16	0.038
	9.0	1.72	0.055
	20.0	2.03	0.067
CTAB	0.4	1.21	0.040
	1.0	1.93	0.090
	3.0	2.15	0.109

^aStandard deviations for the average lifetime (τ_{av}) and anisotropy (r) are ≤ 0.02 ns and 0.002, respectively. ^b r values reported here are blank uncorrected.

Furthermore, a higher fluorescence anisotropy at a surfactant concentration above the cmc as compared to that of an aqueous solution containing a low surfactant concentration indicates that benzothiophene-conjugated uracil is rigidified by the incorporation of the nucleoside within the micellar aggregates (Table 2). On the basis of the above results, it is likely that the benzothiophene-conjugated base is embedded in the hydrocarbon continuum and its hydrophilic sugar moiety is anchored on the micellar surface. Earlier studies have also predicted similar types of interactions with micelles when using probes made of hydrophilic and hydrophobic moieties.^{84,90}

Fluorescence Properties of Ribonucleoside **1** in AOT

RM. The encapsulated water in RM is characterized by a “bound” water close to the interface, which is involved in the hydration of the head groups and counterions, and “free” bulk water in the inner region (Figure 1b).⁹¹ At low water content ($w_0 < 8$), there are fewer water molecules to form a well-defined water pool because most of the water molecules interact with head groups and counterions, forming a domain of structured water that has significantly reduced motion compared to bulk water.⁹¹ As the water–surfactant ratio is increased, a free water pool that exhibits variations in physical parameters (e.g., polarity, viscosity, and water motion) starts to emerge.^{92,93} Typically, an increase in the size of the surfactant-entrapped water pool results in a decrease in the microviscosity and an increase in the micropolarity of the solubilized water.^{58–60} Extensive solvation dynamics studies using ultrafast time-resolved spectroscopy also reveal that the motion of water in RM is significantly slower as compared to that in bulk water.^{94–99}

Several techniques, in particular, fluorescence-based methods, have been utilized in investigating the dynamics, polarity, viscosity, and acid–base reactivity of the confined water as a function of w_0 values.^{54,56–60,100} Most of these methods utilize environment-sensitive fluorescent probes, which have an affinity of one or more of the micellar domains such as the water pool, surfactant interface, or hydrocarbon continuum. While 1,8-anilinonaphthalenesulfonate (ANS), pyrenesulfonic acid (PSA), 1-aminonaphthylene-4-sulfonic acid, rhodamine B, auramine O, and pyranine are solubilized in the aqueous micellar core, amphiphilic pyrene, indole, and tryptophan derivatives are localized in the surfactant interface.⁵⁹ Interestingly, depending on the water loading, prodan has been shown to be present in the inner water pool, AOT interface, and nonpolar solvent phase.^{59,83} Although extensively utilized in several fluorescence assays, these probes are relatively large. Hence, when introduced site-specifically (e.g., site of interaction) into target oligonucleotides, they are likely to perturb the native structure of oligonucleotides. Because benzothiophene-modified ribonucleoside **1** is structurally minimally invasive,⁷² we decided to evaluate the efficacy of the ribonucleoside to sense the environment of AOT RM as a function of w_0 .¹⁰¹

Stock solutions of AOT RM in heptane with increasing w_0 values are prepared by adding appropriate amounts of the

nucleoside stock solutions in water such that the concentration of nucleoside **1** is maintained at 5 μM .^{75,102–104} At low w_0 values (0.7–1.4), the nucleoside shows an intense blue-shifted emission band ($\lambda_{\text{em}} = 432 \text{ nm}$) as compared to the free nucleoside in water ($\lambda_{\text{em}} = 462 \text{ nm}$, Figure 6). When samples

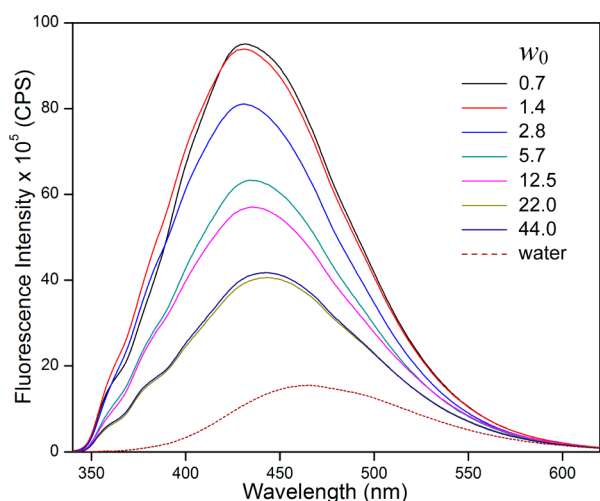


Figure 6. Emission spectra of ribonucleoside **1** (5 μM) in AOT RM as a function of w_0 . Samples were excited at 322 nm, and excitation and emission slit widths were 3 and 5 nm, respectively.⁷⁵

with increasing w_0 values are excited, the nucleoside exhibits significant quenching in fluorescence intensity and a red-shifted emission maximum, which starts to saturate around $w_0 = 22$ (Figure 6). The emission maximum near the saturation point ($\sim 443 \text{ nm}$) is close to the emission maximum of the free nucleoside in methanol (Table 1). Earlier studies using fluorescent dyes that have been used to probe the polarity of AOT RM have also revealed an environment similar to that of methanol in the micellar core.^{105,106} The excited-state decay kinetics of nucleoside **1** has been analyzed by time-resolved fluorescence spectroscopy at varying w_0 values. Upon increasing the water loading, the lifetime decreases progressively and levels off at $w_0 = 22$, which is consistent with the above steady-state fluorescence data (Figure S5, Table S1). Similarly, fluorescence anisotropy measurements indicate that the water pool in RM is very viscous as compared to the free water (Table S1).

The ability of an emissive nucleoside to report the environment of the water pool in RM will depend on the partitioning of the nucleoside in a specific domain at a given w_0 value. On the basis of the above photophysical characterizations, the location of the charge-neutral nucleoside analogue in RM can be predicted. At low water content, a well-defined water pool does not exist, and hence it is likely that the nucleoside resides at the AOT–water interface, which is rigid and less polar. As a result, the nucleoside shows high intensity and a blue-shifted emission maximum. However, as the water content in RM is increased the nucleoside percolates from a more-rigid, less-polar environment to a less-rigid, more-polar water pool. This notion is supported by the fact that the nucleoside exhibits fluorescence quenching, a red-shifted emission maximum, and reduced anisotropy upon increasing the water/AOT molar ratio. Upon performing REES experiments in AOT RM, ribonucleoside **1** exhibits a significant red-shifted emission maximum (11 nm) at $w_0 = 20$ as compared to that at $w_0 = 0$ (Figure S2). This observation indicates the

heterogeneity in the fluorophore–solvent interactions in the confined environment. Because ribonucleoside **1** can report the environment in RM in the form of changes in fluorescence properties such as the fluorescence intensity, emission maximum, lifetime, and anisotropy, we decided to study the photophysical behavior of oligonucleotides labeled with the emissive nucleoside in RM.

Fluorescence Properties of Oligonucleotides Labeled with Ribonucleoside **1 in AOT RM.** The amicability of benzothiophene-modified UTP **2** to enzymatic incorporation allowed the easy synthesis of RNA oligonucleotide **3** containing fluorescent label **1** by in vitro transcription reactions (Figure 7).^{75,107–112} The effect of benzothiophene modification on the

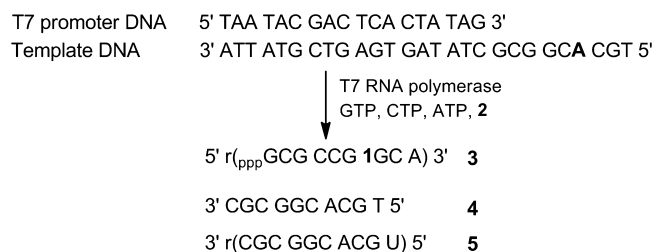


Figure 7. Synthesis of fluorescently modified RNA oligonucleotide **3** by an in vitro transcription reaction in the presence of modified UTP **2** and T7 RNA polymerase.⁷⁵ Sequence of complementary DNA and RNA oligonucleotides **4** and **5**, respectively, used in this study.

hybridization efficiency of oligoribonucleotide **3** was evaluated by performing UV-thermal denaturation and native-gel retardation experiments. The results revealed that the modified oligoribonucleotide formed stable duplexes with complementary oligonucleotides with only a minor reduction in thermal melting temperatures.⁷²

The conformational flexibility and hybridization rates of oligonucleotides have been studied by NMR and UV absorption spectroscopy, respectively, in AOT RM at $w_0 = 20$.^{70,71} Hence, we studied the photophysical behavior of fluorescent RNA oligonucleotide **3** and corresponding complementary RNA–DNA (**3**·**4**) and RNA–RNA (**3**·**5**) duplexes in AOT RM at $w_0 = 20$. Appropriate amounts of the oligonucleotide stock solutions in cacodylate buffer (pH 7.6) were added to AOT RM such that the concentration of the oligonucleotides and w_0 value were maintained at 2 μM and 20, respectively. Upon excitation, RNA oligonucleotide **3** in RM displayed a slightly red-shifted, quenched emission band as compared to the free nucleoside in RM (Figure 8, Table 3, Figure S6). Interestingly, duplexes **3**·**4** and **3**·**5** exhibited discernible enhancements in fluorescence intensity as compared to single-stranded oligoribonucleotide **3**. This observation is uncommon because most of the fluorescent nucleoside analogues, when incorporated into single- and double-stranded oligonucleotides, show significant quenching in fluorescence intensity in aqueous buffers.¹⁴ Consequently, the fluorescence properties of oligonucleotides were also evaluated under similar conditions in aqueous cacodylate buffer. Both single-stranded oligonucleotide and duplexes showed significant fluorescence quenching (4- to 5-fold) in aqueous buffer as compared to that in AOT RM (Figure 8, Table 3, Figure S7). The excited-state lifetime measurements reveal a longer lifetime for oligonucleotides in RM as compared to that in aqueous buffer (Table 3, Figure S8). Furthermore, anisotropy measurements indicate that the motion of the emissive oligonucleotides is considerably

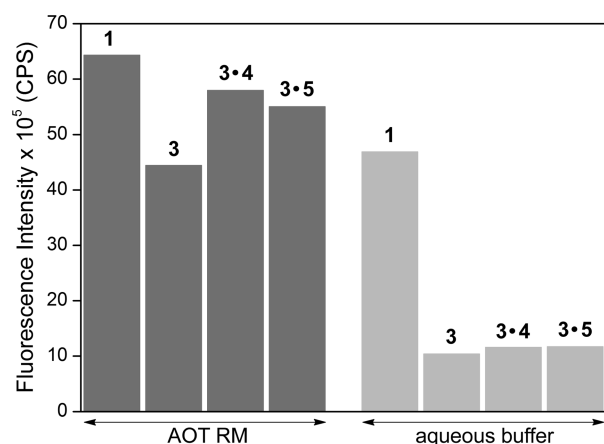


Figure 8. Emission intensity of nucleoside 1, oligoribonucleotide 3, and duplexes of 3 (2 μ M) in AOT RM and aqueous buffer at the respective emission maxima. Samples were excited at 322 nm, and excitation and emission slit widths were 3 and 8 nm, respectively.⁷⁵

Table 3. Fluorescence Properties of 3 and Duplexes Made of 3 in AOT RM and Aqueous Buffer⁷⁵

sample		λ_{em} (nm)	τ_{av} (ns) ^a	$r^{a,b}$
AOT RM	1	442	1.46	0.137
	3	450	1.67	0.171
	3-4	448	1.61	0.174
	3-5	447	1.65	0.174
aqueous buffer	1	465	1.14	0.040
	3	465	1.27	0.101
	3-4	465	1.27	0.101
	3-5	465	1.22	0.105

^aStandard deviations for the average lifetime (τ_{av}) and anisotropy (r) are ≤ 0.05 ns and 0.003, respectively. ^b r values reported here are blank uncorrected.

retarded in AOT RM as opposed to that in aqueous buffer (Table 3).

To confirm if the observed photophysical properties of fluorescently modified oligonucleotide duplexes in AOT RM are due to intact duplexes, we performed UV-thermal melting and circular dichroism (CD) analyses. UV-thermal melting analysis revealed that modified oligoribonucleotide 3 formed stable duplexes with complementary oligonucleotides 4 (45.8 ± 1.0 °C) and 5 (60.5 ± 0.8 °C) in aqueous cacodylate buffer under the conditions used for fluorescence studies. However, a similar analysis could not be performed in AOT RM because the structure of micelles is very sensitive to temperature.^{104,113} Therefore, we performed CD analysis of oligonucleotide duplexes 3-4 and 3-5 in aqueous buffer and AOT RM (Figure S9). The CD spectrum of RNA–DNA duplex 3-4 in aqueous cacodylate buffer displays a positive band centered around 281 nm and a negative band at 251 nm, with a crossover at 263 nm. Although duplex 3-4 in AOT RM ($w_0 = 20$) exhibits no shift in the positive band, it shows a noticeable shift in the negative band to 230 nm. However, RNA–RNA duplex 3-5 displays similar CD profiles in both aqueous buffer and AOT RM, with positive and negative bands at around 274 and 234 nm, respectively. Hence, we believe that the differences in the fluorescence properties of the oligonucleotides in aqueous buffer and RM could be due to the retarded motion and a slight change in the conformation (especially in RNA–DNA duplex) of the intact oligonucleotide duplexes in AOT RM. Moreover,

the higher fluorescence intensity, lifetime, and anisotropy exhibited by fluorescent oligonucleotides in RM are consistent with the environment of the inner core of the water pool in RM, which is less polar and less mobile as compared to those of bulk water. Taken together, these results demonstrate that emissive nucleoside analogue 1 incorporated into oligonucleotides, which can sense the environment of the water pool in RM, can be used to study the dynamics, conformation, and recognition properties of nucleic acids in a model biological compartment.

CONCLUSIONS

We have introduced an environment-sensitive fluorescent nucleoside analogue probe, based on the 5-(benzo[b]-thiophen-2-yl)pyrimidine core, that reports the environment of micelles and RM via changes in its fluorescence properties. The photophysical characterization of the uridine analogue incorporated into oligonucleotides indicates that the motion of oligonucleotides is considerably retarded in RM as compared to that in aqueous buffer, which is in agreement with the environment of the encapsulated water pool in RM. Taken together, emission in the visible region with a reasonable quantum yield, sensitivity to changes in polarity and viscosity, and the ability to report the environment of micelles adequately bestow a probelike attribute to emissive nucleoside 1. These favorable properties of the nucleoside can be potentially utilized in studying the structural dynamics and recognition properties of oligonucleotides in a cell-like confined environment. Efforts to implement this nucleoside analogue in investigating the recognition properties of therapeutically relevant nucleic acid motifs in RM are currently in progress.

ASSOCIATED CONTENT

Supporting Information

Excited-state decay, DLS, and CD profiles and emission spectra of nucleosides. This material is available free of charge via the Internet at <http://pubs.acs.org>.

AUTHOR INFORMATION

Corresponding Author

*E-mail: srivatsan@iiserpune.ac.in. Tel: +91-20-25908086.

Notes

The authors declare no competing financial interest.

ACKNOWLEDGMENTS

We thank the referees and Dr. Partha Hazra of IISER, Pune, for their valuable suggestions. S.G.S thanks the Department of Science and Technology, India (SR/S1/OC-51/2009), and the Council of Scientific and Industrial Research (CSIR), India (02-0086/12/EMR-II), for research grants. S.G.S is grateful to the Alexander von Humboldt foundation for an equipment grant. M.G.P thanks CSIR, India, for a graduate research fellowship.

REFERENCES

- (1) Asseline, U. Development and Applications of Fluorescent Oligonucleotides. *Curr. Org. Chem.* **2006**, *10*, 491–518.
- (2) Martí, A. A.; Jockusch, S.; Stevens, N.; Ju, J.; Turro, N. J. Fluorescent Hybridization Probes for Sensitive and Selective DNA and RNA Detection. *Acc. Chem. Res.* **2007**, *40*, 402–409.
- (3) Hall, K. B. RNA in Motion. *Curr. Opin. Chem. Biol.* **2008**, *12*, 612–618.

- (4) Piton, N.; Mu, Y.; Stock, G.; Prisner, T. F.; Schiemann, O.; Engels, J. W. Base-Specific Spin-Labeling of RNA for Structure Determination. *Nucleic Acids Res.* **2007**, *35*, 3128–3143.
- (5) Aitken, C. E.; Petrov, A.; Puglisi, J. D. Single Ribosome Dynamics and the Mechanism of Translation. *Annu. Rev. Biophys.* **2010**, *39*, 491–513.
- (6) Bardaro, M. F., Jr.; Varani, G. Examining the Relationship between RNA Function and Motion Using Nuclear Magnetic Resonance. *WIREs RNA* **2012**, *3*, 122–132.
- (7) Nguyen, P.; Qin, P. Z. RNA Dynamics: Perspectives from Spin Labels. *WIREs RNA* **2012**, *3*, 62–72.
- (8) Ogle, J. M.; Carter, A. P.; Ramakrishnan, V. Insights into the Decoding Mechanism from Recent Ribosome Structures. *Trends Biochem. Sci.* **2003**, *28*, 259–266.
- (9) Korostelev, A.; Trakhanov, S.; Laurberg, M.; Noller, H. F. Crystal Structure of a 70S Ribosome tRNA Complex Reveals Functional Interactions and Rearrangements. *Cell* **2006**, *126*, 1065–1077.
- (10) Serganov, A.; Patel, D. J. Molecular Recognition and Function of Riboswitches. *Curr. Opin. Struct. Biol.* **2012**, *22*, 279–286.
- (11) Ranasinghe, R. T.; Brown, T. Fluorescence Based Strategies for Genetic Analysis. *Chem. Commun.* **2005**, 5487–5502.
- (12) Shi, X.; Herschlag, D. Fluorescence Polarization Anisotropy to Measure RNA Dynamics. *Methods Enzymol.* **2009**, *469*, 287–302.
- (13) Wilson, J. N.; Kool, E. T. Fluorescent DNA Base Replacements: Reporters and Sensors for Biological Systems. *Org. Biomol. Chem.* **2006**, *4*, 4265–4274.
- (14) Sinkeldam, R. W.; Greco, N. J.; Tor, Y. Fluorescent Analogs of Biomolecular Building Blocks: Design, Properties, and Applications. *Chem. Rev.* **2010**, *110*, 2579–2619.
- (15) Wilhelmsson, L. M. Fluorescent Nucleic Acid Base Analogues. *Q. Rev. Biophys.* **2010**, *43*, 159–183.
- (16) Srivatsan, S. G.; Sawant, A. A. Fluorescent Ribonucleoside Analogues as Probes for Investigating RNA Structure and Function. *Pure Appl. Chem.* **2011**, *83*, 213–232.
- (17) Phelps, K.; Morris, A.; Beal, P. A. Novel Modifications in RNA. *ACS Chem. Biol.* **2012**, *7*, 100–109.
- (18) Okamoto, A.; Saito, Y.; Saito, I. Design of Base-Discriminating Fluorescent Nucleosides. *J. Photochem. Photobiol. C* **2005**, *6*, 108–122.
- (19) Mayer-Enthart, E.; Wagenknecht, H.-A. Structure-Sensitive and Self-Assembled Helical Pyrene Array Based on DNA Architecture. *Angew. Chem., Int. Ed.* **2006**, *45*, 3372–3375.
- (20) Tainaka, K.; Tanaka, K.; Ikeda, S.; Nishiza, K.-I.; Unzai, T.; Fujiwara, Y.; Saito, I.; Okamoto, A. PRODAN-Conjugated DNA: Synthesis and Photochemical Properties. *J. Am. Chem. Soc.* **2007**, *129*, 4776–4784.
- (21) Xiao, Q.; Ranasinghe, R. T.; Tang, A. M. P.; Brown, T. Naphthalenyl- and Anthracenyl-ethynyl dT Analogues as Base Discriminating Fluorescent Nucleosides and Intramolecular Energy Transfer Donors in Oligonucleotide Probes. *Tetrahedron* **2007**, *63*, 3483–3490.
- (22) Srivatsan, S. G.; Weizman, H.; Tor, Y. A Highly Fluorescent Nucleoside Analog Based on Thieno[3,4-*d*]pyrimidine Senses Mismatched Pairing. *Org. Biomol. Chem.* **2008**, *6*, 1334–1338.
- (23) Gardarsson, H.; Kale, A. S.; Sigurdsson, S. T. Structure–Function Relationships of Phenoxazine Nucleosides for Identification of Mismatches in Duplex DNA by Fluorescence Spectroscopy. *ChemBioChem* **2011**, *12*, 567–575.
- (24) Shipova, E.; Gates, K. S. A Fluorimetric Assay for the Spontaneous Release of an N7-Alkylguanine Residue from Duplex DNA. *Bioorg. Med. Chem. Lett.* **2005**, *15*, 2111–2113.
- (25) Greco, N. J.; Sinkeldam, R. W.; Tor, Y. An Emissive C Analog Distinguishes between G, 8-oxoG, and T. *Org. Lett.* **2009**, *11*, 1115–1118.
- (26) Srivatsan, S. G.; Greco, N. J.; Tor, Y. A Highly Emissive Fluorescent Nucleoside That Signals the Activity of Toxic Ribosome-Inactivating Proteins. *Angew. Chem., Int. Ed.* **2008**, *47*, 6661–6665.
- (27) Hirose, W.; Sato, K.; Matsuda, A. Selective Detection of 5-Formyl-2'-deoxyuridine, an Oxidative Lesion of Thymidine, in DNA by a Fluorogenic Reagent. *Angew. Chem., Int. Ed.* **2010**, *49*, 8392–8394.
- (28) Parsons, J.; Castaldi, M. P.; Dutta, S.; Dibrov, S. M.; Wyles, D. L.; Hermann, T. Conformational Inhibition of the Hepatitis C Virus Internal Ribosome Entry Site RNA. *Nat. Chem. Biol.* **2009**, *5*, 823–825.
- (29) Nadler, A.; Strohmeier, J.; Diederichsen, U. 8-Vinyl-2'-deoxyguanosine as a Fluorescent 2'-Deoxyguanosine Mimic for Investigating DNA Hybridization and Topology. *Angew. Chem., Int. Ed.* **2011**, *50*, 5392–5396.
- (30) Lee, J. II; Kim, B. H. Monitoring i-Motif Transitions through the Exciplex Emission of a Fluorescent Probe Incorporating Two ¹⁹A units. *Chem. Commun.* **2012**, *48*, 2074–2076.
- (31) Rieder, R.; Lang, K.; Graber, D.; Micura, R. Ligand-Induced Folding of the Adenosine Deaminase A-Riboswitch and Implications on Riboswitch Translational Control. *ChemBioChem* **2007**, *8*, 896–902.
- (32) Xie, Y.; Dix, A. V.; Tor, Y. FRET Enabled Real Time Detection of RNA-Small Molecule Binding. *J. Am. Chem. Soc.* **2009**, *131*, 17605–17614.
- (33) Wahba, A. S.; Esmaeili, A.; Damha, M. J.; Hudson, R. H. E. A Single-Label Phenylpyrrolocytidine Provides a Molecular Beacon-like Response Reporting HIV-1 RT RNase H Activity. *Nucleic Acids Res.* **2010**, *38*, 1048–1056.
- (34) Riedl, J.; Pohl, R.; Ernsting, N. P.; Ors  g, P.; Fojta, M.; Hocek, M. Labelling of Nucleosides and Oligonucleotides by Solvatochromic 4-Aminophthalimide Fluorophore for Studying DNA–Protein Interactions. *Chem. Sci.* **2012**, *3*, 2797–2806.
- (35) Pawar, M. G.; Nuthanakanti, A.; Srivatsan, S. G. Heavy Atom Containing Fluorescent Ribonucleoside Analog Probe for the Fluorescence Detection of RNA-Ligand Binding. *Bioconjugate Chem.* **2013**, *24*, 1367–1377.
- (36) Kelley, S. O.; Barton, J. K. Electron Transfer Between Bases in Double Helical DNA. *Science* **1999**, *283*, 375–381.
- (37) Grigorenko, N. A.; Leumann, C. J. Electron Transfer through a Stable Phenanthrenyl Pair in DNA. *Chem. Commun.* **2008**, 5417–5419.
- (38) Murphy, L. D.; Zimmerman, S. B. Macromolecular Crowding Effects on the Interaction of DNA with *Escherichia coli* DNA-Binding Proteins: A Model for Bacterial Nucleoid Stabilization. *Biochim. Biophys. Acta* **1994**, *1219*, 277–284.
- (39) Ellis, R. J. Macromolecular Crowding: An Important but Neglected Aspect of the Intracellular Environment. *Curr. Opin. Struct. Biol.* **2001**, *11*, 114–119.
- (40) Flynn, P. F. Multidimensional Multinuclear Solution NMR Studies of Encapsulated Macromolecules. *Prog. Nucl. Magn. Reson. Spectrosc.* **2004**, *45*, 31–51.
- (41) Snoussi, K.; Halle, B. Protein Self-Association Induced by Macromolecular Crowding: A Quantitative Analysis by Magnetic Relaxation Dispersion. *Biophys. J.* **2005**, *88*, 2855–2866.
- (42) Minton, A. P. Influence of Macromolecular Crowding upon the Stability and State of Association of Proteins: Predictions and Observations. *J. Pharm. Sci.* **2005**, *94*, 1668–1675.
- (43) Luisi, P. L.; Giomini, M.; Pileni, M. P.; Robinson, B. H. Reverse Micelles as Hosts for Proteins and Small Molecules. *Biochim. Biophys. Acta* **1988**, *947*, 209–246.
- (44) Bru, R.; S  nchez-Ferrer, A.; Garc  a-Carmona, F. Kinetic Models in Reverse Micelles. *Biochem. J.* **1995**, *310*, 721–739.
- (45) Levinger, N. E. Water in Confinement. *Science* **2002**, *298*, 1722–1723.
- (46) Effects of crowding and confinement on the structure and activity of biomacromolecules, especially proteins, have been studied in RM. Visser, A. J. W. G.; Fendler, J. H. Reduction of Reversed Micelle Entrapped Cytochrome *c* and Cytochrome *c*₃ by Electrons Generated by Pulse Radiolysis or by Pyrene Photoionization. *J. Phys. Chem.* **1982**, *86*, 947–950. See also refs 47–52.
- (47) Shastry, M. C. R.; Eftink, M. R. Reversible Thermal Unfolding of Ribonuclease T₁ in Reverse Micelles. *Biochemistry* **1996**, *35*, 4094–4101.

- (48) Das, P. K.; Chaudhuri, A. On the Origin of Unchanged Lipase Activity Profile in Cationic Reverse Micelles. *Langmuir* **2000**, *16*, 76–80.
- (49) Uskova, M. A.; Borst, J.-W.; Hink, M. A.; van Hoek, A.; Schots, A.; Klyachko, N. L.; Visser, A. J. W. G. Fluorescence Dynamics of Green Fluorescent Protein in AOT Reversed Micelles. *Biophys. Chem.* **2000**, *87*, 73–84.
- (50) Airoldi, M.; Boicelli, C. A.; Gennaro, G.; Giomini, M.; Giuliani, A. M.; Giustini, M.; Scibetta, L. Different Factors Affecting PolyAT Conformation in Microemulsions: Effects of Variable P_0 and KCl Concentration. *Phys. Chem. Chem. Phys.* **2002**, *4*, 3859–3864.
- (51) Shi, Z.; Peterson, R. W.; Wand, A. J. New Reverse Micelle Surfactant Systems Optimized for High-Resolution NMR Spectroscopy of Encapsulated Proteins. *Langmuir* **2005**, *21*, 10632–10637.
- (52) Van Horn, W. D.; Ogilvie, M. E.; Flynn, P. F. Reverse Micelle Encapsulation as a Model for Intracellular Crowding. *J. Am. Chem. Soc.* **2009**, *131*, 8030–8039.
- (53) De, T. K.; Maitra, A. Solution Behaviour of Aerosol OT in Non-polar Solvents. *Adv. Colloid Interface Sci.* **1995**, *59*, 95–193.
- (54) Silber, J. J.; Biasutti, A.; Abuin, E.; Lissi, E. Interactions of Small Molecules with Reverse Micelles. *Adv. Colloid Interface Sci.* **1999**, *82*, 189–252.
- (55) Fletcher, P. D. I.; Howe, A. M.; Robinson, B. H. The Kinetics of Solubilisation Exchange between Water Droplets of a Water-in-Oil Microemulsion. *J. Chem. Soc., Faraday Trans. 1* **1987**, *83*, 985–1006.
- (56) Nandi, N.; Bhattacharyya, K.; Bagchi, B. Dielectric Relaxation and Solvation Dynamics of Water in Complex Chemical and Biological Systems. *Chem. Rev.* **2000**, *100*, 2013–2045.
- (57) Levinger, N. E.; Swafford, L. A. Ultrafast Dynamics in Reverse Micelles. *Annu. Rev. Phys. Chem.* **2009**, *60*, 385–406.
- (58) Correa, N. M.; Biasutti, M. A.; Silber, J. J. Micropolarity of Reverse Micelles of Aerosol-OT in *n*-Hexane. *J. Colloid Interface Sci.* **1995**, *172*, 71–76.
- (59) Karukstis, K. K.; Frazier, A. A.; Martula, D. S.; Whiles, J. A. Characterization of the Microenvironments in AOT Reverse Micelles Using Multidimensional Spectral Analysis. *J. Phys. Chem.* **1996**, *100*, 11133–11138.
- (60) Hasegawa, M.; Sugimura, T.; Suzuki, Y.; Shindo, Y. Microviscosity in Water Pool of Aerosol-OT Reversed Micelle Determined with Viscosity-Sensitive Fluorescence Probe, Auramine O, and Fluorescence Depolarization of Xanthene Dyes. *J. Phys. Chem.* **1994**, *98*, 2120–2124.
- (61) Politi, M. J.; Chaimovich, H. Water Activity in Reversed Sodium Bis(2-ethylhexyl) Sulfosuccinate Micelles. *J. Phys. Chem.* **1986**, *90*, 282–287.
- (62) Mukherjee, T. K.; Panda, D.; Datta, A. Excited-State Proton Transfer of 2-(2'-Pyridyl)benzimidazole in Microemulsions: Selective Enhancement and Slow Dynamics in Aerosol OT Reverse Micelles with an Aqueous Core. *J. Phys. Chem. B* **2005**, *109*, 18895–18901.
- (63) Luisi, P. L.; Magid, L. J. Solubilization of Enzymes and Nucleic Acids in Hydrocarbon Micellar Solutions. *CRC Crit. Rev. Biochem.* **1986**, *20*, 409–474.
- (64) Ijio, K.; Okahata, Y. A DNA-Lipid Complex Soluble in Organic Solvents. *J. Chem. Soc., Chem. Commun.* **1992**, 1339–1341.
- (65) Mel'nikov, S. M.; Lindman, B. Solubilization of DNA-Cationic Lipid Complexes in Hydrophobic Solvents. A Single-Molecule Visualization by Fluorescence Microscopy. *Langmuir* **1999**, *15*, 1923–1928.
- (66) Budker, V. G.; Slattum, P. M.; Monahan, S. D.; Wolff, J. A. Entrapment and Condensation of DNA in Neutral Reverse Micelles. *Biophys. J.* **2002**, *82*, 1570–1579.
- (67) Shaw, A. K.; Sarkar, R.; Pal, S. K. Direct Observation of DNA Condensation in a Nano-Cage by Using a Molecular Ruler. *Chem. Phys. Lett.* **2005**, *408*, 366–370.
- (68) Sarkar, R.; Pal, S. K. Ligand–DNA Interaction in a Nanocage of Reverse Micelle. *Biopolymers* **2006**, *83*, 675–686.
- (69) Nezhad, E. H.; Ghorbani, M.; Zeinalkhani, M.; Heidari, A. DNA Encapsulation in an Anionic Reverse Micellar Solution of Dioctyl Sodium Sulfosuccinate. *Phys. Chem.* **2013**, *3*, 7–10.
- (70) Park, L.-C.; Maruyama, T.; Goto, M. DNA Hybridization in Reverse Micelles and its Application to Mutation Detection. *Analyst* **2003**, *128*, 161–165.
- (71) Workman, H.; Flynn, P. F. Stabilization of RNA Oligomers through Reverse Micelle Encapsulation. *J. Am. Chem. Soc.* **2009**, *131*, 3806–3807.
- (72) Pawar, M. G.; Srivatsan, S. G. Synthesis, Photophysical Characterization, and Enzymatic Incorporation of a Microenvironment Sensitive Fluorescent Uridine Analog. *Org. Lett.* **2011**, *13*, 1114–1117.
- (73) Bahri, M. A.; Hoebeke, M.; Grammenos, A.; Delanaye, L.; Vandewalle, N.; Seret, A. Investigation of SDS, DTAB and CTAB Micelle Microviscosities by Electron Spin Resonance. *Colloids Surf., A* **2006**, *290*, 206–212.
- (74) Aguiar, J.; Carpena, P.; Molina-Bolívar, J. A.; Carnero Ruiz, C. On the Determination of the Critical Micelle Concentration by the Pyrene 1:3 Ratio Method. *J. Colloid Interface Sci.* **2003**, *258*, 116–122.
- (75) See the Experimental Section for details.
- (76) Tanpure, A. A.; Pawar, M. G.; Srivatsan, S. G. Fluorescent Nucleoside Analogs: Probes for Investigating Nucleic Acid Structure and Function. *Isr. J. Chem.* **2013**, *53*, 366–378.
- (77) Reichardt, C. Solvatochromic Dyes as Solvent Polarity Indicators. *Chem. Rev.* **1994**, *94*, 2319–2358.
- (78) Demchenko, A. P. On the Nanosecond Mobility in Proteins: Edge Excitation Fluorescence Red Shift of Protein-Bound 2-(*p*-Toluidinylnaphthalene)-6-Sulfonate. *Biophys. Chem.* **1982**, *15*, 101–109.
- (79) Lakowicz, J. R.; Keating-Nakamoto, S. Red-Edge Excitation of Fluorescence and Dynamic Properties of Proteins and Membranes. *Biochemistry* **1984**, *23*, 3013–3021.
- (80) Macgregor, R. B.; Weber, G. Estimation of the Polarity of the Protein Interior by Optical Spectroscopy. *Nature* **1986**, *319*, 70–73.
- (81) Chattopadhyay, A.; Mukherjee, S. Fluorophore Environments in Membrane-Bound Probes: A Red Edge Excitation Shift Study. *Biochemistry* **1993**, *32*, 3804–3811.
- (82) Dennison, S. M.; Guharay, J.; Sengupta, P. K. *Spectrochim. Acta A* **1999**, *55*, 1127–1132.
- (83) Sengupta, B.; Guharay, J.; Sengupta, P. K. Characterization of the Fluorescence Emission Properties of Prodan in Different Reverse Micellar Environments. *Spectrochim. Acta A* **2000**, *56*, 1433–1441.
- (84) Kalyanasundaram, K.; Thomas, J. K. Solvent-Dependent Fluorescence of Pyrene-3-carboxaldehyde and Its Applications in the Estimation of Polarity at Micelle-Water Interfaces. *J. Phys. Chem.* **1977**, *81*, 2176–2180.
- (85) Ananthapadmanabhan, K. P.; Goddard, E. D.; Turro, N. J.; Kuo, P. L. Fluorescence Probes for Critical Micelle Concentration. *Langmuir* **1985**, *1*, 352–355.
- (86) Karukstis, K. K.; Suljak, S. W.; Waller, P. J.; Whiles, J. A.; Thompson, E. H. Z. Fluorescence Analysis of Single and Mixed Micelle Systems of SDS and DTAB. *J. Phys. Chem.* **1996**, *100*, 11125–11132.
- (87) Shiota, H.; Tamoto, Y.; Segawa, H. Dynamic Fluorescence Probing of the Microenvironment of Sodium Dodecyl Sulfate Micelle Solutions: Surfactant Concentration Dependence and Solvent Isotope Effect. *J. Phys. Chem. A* **2004**, *108*, 3244–3252.
- (88) Chaudhuri, A.; Haldar, S.; Chattopadhyay, A. Organization and Dynamics in Micellar Structural Transition Monitored by Pyrene Fluorescence. *Biochem. Biophys. Res. Commun.* **2009**, *390*, 728–732.
- (89) Mohr, A.; Talbiersky, P.; Korth, H.-G.; Sustmann, R.; Boese, R.; Bläser, D.; Rehage, H. A New Pyrene-Based Fluorescent Probe for the Determination of Critical Micelle Concentrations. *J. Phys. Chem. B* **2007**, *111*, 12985–12992.
- (90) Fendler, J. H.; Fendler, E. J.; Infante, G. A.; Shih, P.-S.; Patterson, L. K. Absorption and Proton Magnetic Resonance Spectroscopic Investigation of the Environment of Acetophenone and Benzophenone in Aqueous Micellar Solutions. *J. Am. Chem. Soc.* **1975**, *97*, 89–95.
- (91) Zinsli, P. E. Inhomogeneous Interior of Aerosol OT Microemulsions Probed by Fluorescence and Polarization Decay. *J. Phys. Chem.* **1979**, *83*, 3223–3231.

- (92) Wong, M.; Thomas, J. K.; Grätzel, M. Fluorescence Probing of Inverted Micelles. The State of Solubilized Water Clusters in Alkane/Diisooctyl Sulfosuccinate (Aerosol OT) Solution. *J. Am. Chem. Soc.* **1976**, *98*, 2391–2397.
- (93) Fulton, J. L.; Blitz, J. P.; Tingey, J. M.; Smith, R. D. Reverse Micelle and Microemulsion Phases in Supercritical Xenon and Ethane: Light Scattering and Spectroscopic Probe Studies. *J. Phys. Chem.* **1989**, *93*, 4198–4204.
- (94) Even at w_0 value as high as 40 the properties of the water pool are discernibly different than those of the continuous aqueous solution. See ref 92.
- (95) Zhang, J.; Bright, F. V. Nanosecond Reorganization of Water within the Interior of Reversed Micelles Revealed by Frequency-Domain Fluorescence Spectroscopy. *J. Phys. Chem.* **1991**, *95*, 7900–7907.
- (96) Onori, G.; Santucci, A. IR Investigations of Water Structure in Aerosol OT Reverse Micellar Aggregates. *J. Phys. Chem.* **1993**, *97*, 5430–5434.
- (97) Sarkar, N.; Das, K.; Datta, A.; Das, S.; Bhattacharyya, K. Solvation Dynamics of Coumarin 480 in Reverse Micelles. Slow Relaxation of Water Molecules. *J. Phys. Chem.* **1996**, *100*, 10523–10527.
- (98) Das, S.; Datta, A.; Bhattacharyya, K. Deuterium Isotope Effect on 4-Aminophthalimide in Neat Water and Reverse Micelles. *J. Phys. Chem. A* **1997**, *101*, 3299–3304.
- (99) Riter, R. E.; Undiks, E. P.; Levinger, N. E. Impact of Counterion on Water Motion in Aerosol OT Reverse Micelles. *J. Am. Chem. Soc.* **1998**, *120*, 6062–6067.
- (100) Behera, G. B.; Mishra, B. K.; Behera, P. K.; Panda, M. Fluorescent Probes for Structural and Distance Effect Studies in Micelles, Reversed Micelles and Microemulsions. *Adv. Colloid Interface Sci.* **1999**, *82*, 1–42.
- (101) 2-Aminopurine, a fluorescent analog of adenine, has been used as a donor to construct FRET pairs in RM. Ghatak, C.; Rao, V. G.; Mandal, S.; Pramanik, R.; Sarkar, S.; Verma, P. K.; Sarkar, N. Förster Resonance Energy Transfer Among a Structural Isomer of Adenine and Various Coumarins Inside a Nanosized Reverse Micelle. *Spectrochim. Acta A* **2012**, *89*, 67–73.
- (102) The size of AOT RM in the absence and presence of nucleoside **1** determined by using dynamic light scattering (DLS) is in good agreement with literature reports (Figure S4). See also refs 103 and 104.
- (103) Riter, R. E.; Kimmel, J. R.; Undiks, E. P.; Levinger, N. E. Novel Reverse Micelles Partitioning Nonaqueous Polar Solvents in a Hydrocarbon Continuous Phase. *J. Phys. Chem. B* **1997**, *101*, 8292–8297.
- (104) Mitra, R. K.; Sinha, S. S.; Pal, S. K. Temperature-Dependent Solvation Dynamics of Water in Sodium Bis(2-ethylhexyl)-sulfosuccinate/Isooctane Reverse Micelles. *Langmuir* **2008**, *24*, 49–56.
- (105) Belletête, M.; Lachapelle, M.; Durocher, G. Polarity of AOT Micellar Interfaces: Use of the Preferential Solvation Concepts in the Evaluation of the Effective Dielectric Constants. *J. Phys. Chem.* **1990**, *94*, 5337–5341.
- (106) Hazra, P.; Sarkar, N. Intramolecular Charge Transfer Processes and Solvation Dynamics of Coumarin 490 in Reverse Micelles. *Chem. Phys. Lett.* **2001**, *342*, 303–311.
- (107) Enzymatic methods have been effectively used to synthesize fluorescently modified oligonucleotides. Lang, K.; Rieder, R.; Micura, R. Ligand-Induced Folding of the *thiM* TPP Riboswitch Investigated by a Structure-Based Fluorescence Spectroscopic Approach. *Nucleic Acids Res.* **2007**, *35*, 5370–5378. See refs 108–112.
- (108) Srivatsan, S. G.; Tor, Y. Enzymatic Incorporation of Emissive Pyrimidine Ribonucleotides. *Chem. Asian J.* **2009**, *4*, 419–427.
- (109) Kimoto, M.; Mitsui, T.; Yokoyama, S.; Hirao, I. A Unique Fluorescent Base Analogue for the Expansion of the Genetic Alphabet. *J. Am. Chem. Soc.* **2010**, *132*, 4988–4989.
- (110) Tanpure, A. A.; Srivatsan, S. G. A Microenvironment-Sensitive Fluorescent Pyrimidine Ribonucleoside Analogue: Synthesis, Enzymatic Incorporation, and Fluorescence Detection of a DNA Abasic Site. *Chem.—Eur. J.* **2011**, *17*, 12820–12827.
- (111) Riedl, J.; Ménová, P.; Pohl, R.; Orság, P.; Fojta, M.; Hocek, M. GFP-like Fluorophores as DNA Labels for Studying DNA–Protein Interactions. *J. Org. Chem.* **2012**, *77*, 8287–8293.
- (112) Holzberger, B.; Strohmeier, J.; Siegmund, V.; Diederichsen, U.; Marx, A. Enzymatic Synthesis of 8-Vinyl- and 8-styryl-2'-deoxyguanosine Modified DNA—Novel Fluorescent Molecular Probes. *Bioorg. Med. Chem. Lett.* **2012**, *22*, 3136–3139.
- (113) Mitra, R. K.; Paul, B. K. Effect of NaCl and Temperature on the Water Solubilization Behavior of AOT/Nonionics Mixed Reverse Micellar Systems Stabilized in IPM Oil. *Colloids Surf. A* **2005**, *255*, 165–180.